Dynamics of an athermal binary mixture of active and passive particles

Pritha Dolai, Aditi Simha and Shradha Mishra

August 4, 2017

Outline

- Active matter
- Equilibrium binary mixture
- Motivation
- Model
- Results
- Summary

Active Systems

- Composed of large number of active agents, each of which consumes energy in order to move or to exert mechanical forces.
- Due to energy consumption, these systems are intrinsically out of equilibrium.

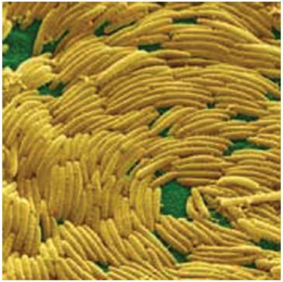

Figure: Liquid crystalline order in a mixobacterial flock. Ref: Rev. Mod. Phys. 2013, **85**, 1143 .

Figure: A school of fish, illustrating local parallel alignment but global vortex. Figure taken from google images.

Phase separation of self-propelled particles

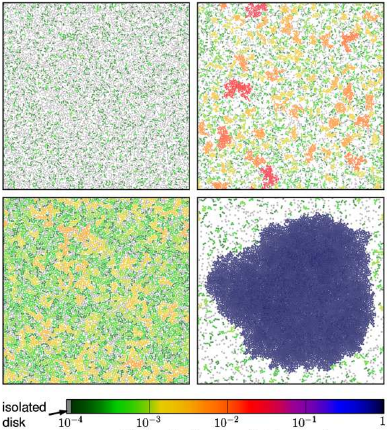

FIG. 1 (color online). Snapshots of $N_T = 10^4$ disks for $\phi = 0.39$ (top row) and $\phi = 0.7$ (bottom row). Same-size clusters, defined by particles overlap, are highlighted by color coding. The left frames are for a thermal system at $k_B T = 0.1$. The right frames are for SP disks with $v_0 = 1$ and $\nu_r = 5 \times 10^{-3}$.

Ref: Y. Fily and M. Cristina Marchetti, PRL, **108**, 235702 (2012)

Equilibrium binary mixtures: depletion effect

- Dense asymmetric binary mixture of hard spheres phase separate for size ratio greater than 5 [T. Biben and J.P. Hansen, PRL (1991)] .
- Depletion effect causes demixing in the hard sphere mixtures: entropy driven phase separation.
- There exist a first-order, entropy-driven demixing transition in a simple lattice model for a hard-core mixture [D. Frenkel and Ard A. Louis, PRL (1992)] .

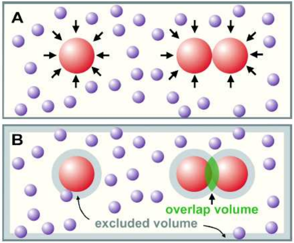

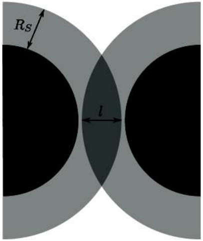

Binary mixture of active and passive particles

- *S*ystem: Asymmetric binary mixtures of active and passive particles on a two dimensional substrate.
- All interactions - soft and repulsive.
- No translational noise (athermal).
- How is the active particle dynamics influenced by the passive beads?
- How do the passive particles behave in the presence of active particles?

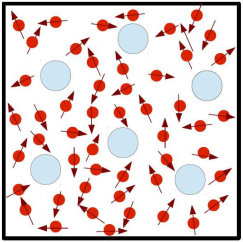

Governing equations

- Equations of motion of active particles

$$\partial_t \mathbf{r}_i = v_1 \hat{\boldsymbol{\nu}}_i + \mu_1 \sum_{i \neq j} \mathbf{F}^1_{ij}\,, \;\; \partial_t \theta_i = \eta^r_i(t)\,. \tag{1}$$

- $\hat{\boldsymbol{\nu}}_i = (cos\theta_i, sin\theta_i)\,, < \eta^r_i(t)\eta^r_j(t') >= 2\nu_r \delta_{ij}\delta(t - t')$.

- Equation of motion of passive particles

$$\partial_t \mathbf{r}_i = \mu_2 \sum_{i \neq j} \mathbf{F}^2_{ij}\,. \tag{2}$$

- Particles are athermal.

- $\mathbf{F}_{ij} = F_{ij}\hat{\mathbf{r}}_{ij}$ with $F_{ij} = k(\sigma_i + \sigma_j - r_{ij})$ if $r_{ij} \leq \sigma_i + \sigma_j$ and $F_{ij} = 0$ otherwise where $r_{ij} = |\mathbf{r}_i - \mathbf{r}_j|$.

Length scale and time scales

- Length scale: radius of each active particle (σ_1).
- Three time scales in the system.
- Angular time scale: ν_r^{-1}, time to change orientation of active particles.
- Elastic time scale: $(\mu k)^{-1}$.
- Collisional time scale: $(2\sigma_1 v_1 \rho)^{-1}$ with $\rho = N_s/L^2$.
- Angular Peclet number: $v_1/\sigma_1\nu_r$.
- Scaled activity: $v_0 = v_1/\sigma_1\mu_1 k$.
- Size ratio: $s = \sigma_2/\sigma_1$.

Dilute phase: Velocity distributions

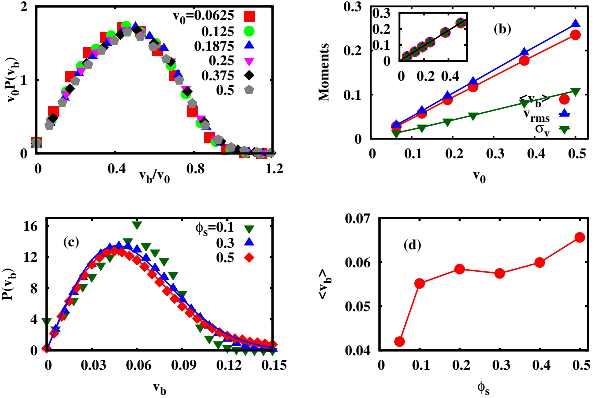

Figure: (a) $P(v_b)$ in dilute phase $\phi_s = \phi_b = 0.1$ for fixed size ratio $s = 6$. (b) Corresponding average velocity $< v_b >$, rms velocity v_{rms} and standard deviation σ_v as a function of activity. (c) $P(v_b)$ for different ϕ_s at fixed activity $v_0 = 0.125$, $s = 5$ and $\phi_b = 0.076$. (d) Corresponding average velocity $< v_b >$ as a function of ϕ_s.

- $P(v_b)$ scales with activity.
- $< v_b >$, v_{rms} and σ_v scale linearly with activity.
- $P(v_b)$ fits well to the Maxwell Boltzmann distribution for intermediate ϕ_s (like 0.3).

Clustering of active particles

- Passive particles enhance the aggregation of active particles.
- It increase the effective volume fraction of active particles.

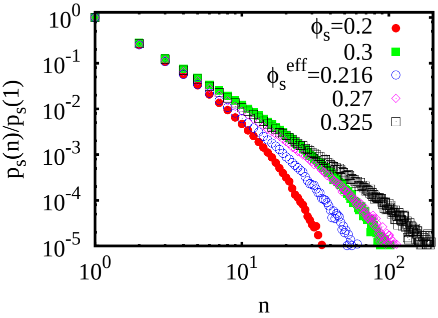

Figure: CSD of a pure active system of $\phi_s = 0.2$, 0.3 (filled symbols) and that of active particles in a mixture of active and passive particles with $\phi_s = 0.2$, 0.25 , 0.3 (open symbols) and $\phi_b = 0.076$ at fixed activity $v_0 = 0.125$.

- The passive particles, being slower than active particles act as nucleation sites where motility induced clustering of active particles can occur.

Number fluctuations

$$\Delta N_s^2 \sim N_s^{\alpha}\ ,\ \ \Delta N_b^2 \sim N_b^{\beta}\ . \tag{3}$$

ϕ_s	ϕ_b	α	β
0.4	0.1	1.35±0.02	1.0±0.01
0.45	0.1	1.44±0.04	1.08±0.02
0.5	0.05	1.53±0.03	1.05±0.02
0.5	0.1	1.55±0.03	1.11±0.02
0.5	0.2	1.55±0.03	1.22±0.03

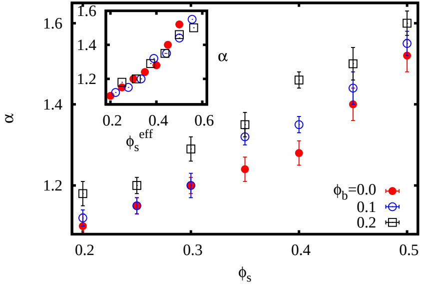

- α increases on increasing ϕ_b due to increased effective volume fraction.
- Passive particles also exhibit giant number fluctuations for sufficiently large ϕ_s (> 0.4).

Diffusivities of passive particles

- MSD indicates a ballistic phase at small times and diffusive behaviour at long times.
- Diffusivity increases nearly linearly with size for small size ratios.
- Scales with the activity.

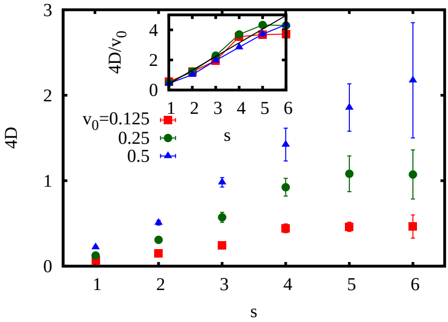

Figure: Diffusivities as a function of size ratio for different activities of active particles at fixed volume fractions $\phi_s = 0.3$ and $\phi_b = 0.1$.

- At large size ratios, there seems to be a decrease with respect to the linear dependence for smaller activities.

Dense phase: Effective interactions

- Radial distribution functions (RDF) are calculated between pairs of particles.
- Beyond a critical ϕ_s , the second peak in $g_{bb}(r)$ dominates over the first peak.
- Peaks broaden as ϕ_s increases.

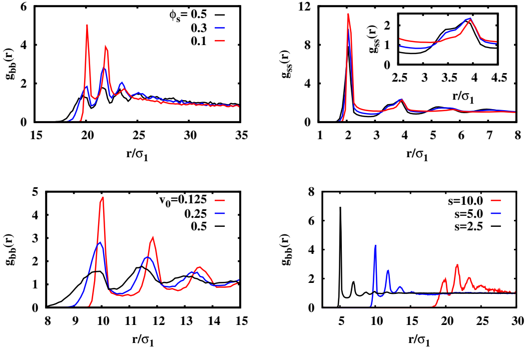

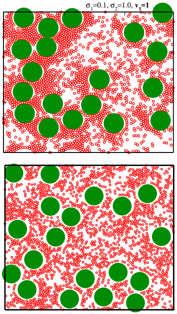

- As activity increases the first peak in $g_{bb}(r)$ broadens indicating the existence of greater attractive force between two big particles.

Radial distribution functions

- As asymmetry increases, peaks become broader and shorter.

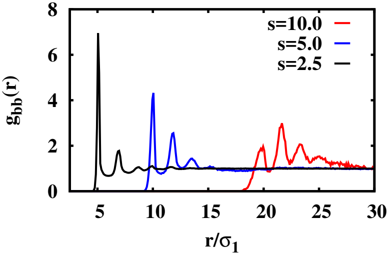

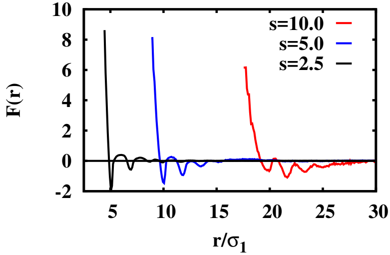

- 2nd peak in $g_{bb}(r)$ dominates when particles are more asymmetric.
- There is a finite probability of finding two big particles together when the distance between them is less than $2\sigma_2$ which confirms that there is an attraction.

Snapshots for different size ratios

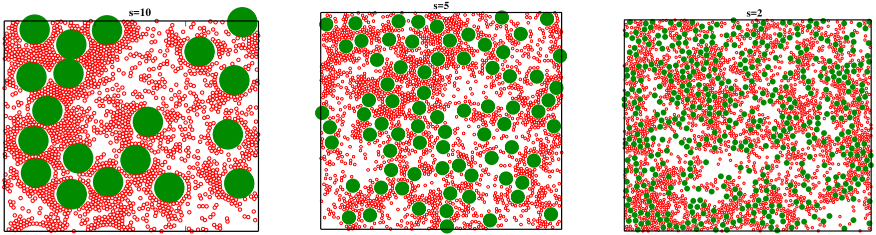

Figure: Snapshot for $s = 10$ (left), $s = 5$ (middle) and $s = 2$ (right) for fixed volume fractions $\phi_s = \phi_b = 0.3$ and activity $v_0 = 0.125$.

Phase diagram

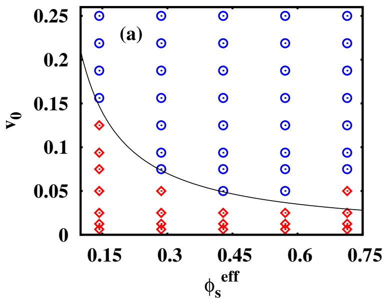

Figure: A phase diagram for $s = 10$ and 5 . Blue circles ($\odot$) and red diamonds ($\diamond$) represent the case when 2nd peak in $g_{bb}(r)$ is larger and smaller than the first peak respectively.

Velocity distributions of active particles

- $P(v_s)$ has a very sharp peak at its self-propulsion speed.
- A small hump appears at small velocities indicating the presence of less mobile clusters of active particles in the system.

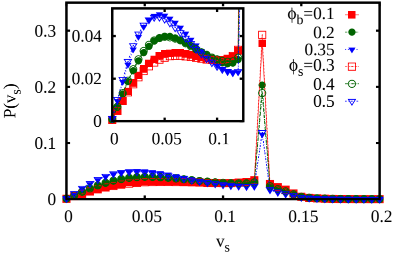

ϕ_s	ϕ_b	ϕ_s^{eff}
0.3	0.1	0.333
0.3	0.2	0.375
0.3	0.35	0.4615
0.3	0.076	0.325
0.4	0.076	0.433
0.5	0.076	0.541

- The curves for $\phi_s = 0.4$, $\phi_b = 0.076$ and $\phi_s = 0.3$, $\phi_b = 0.2$ overlap. The latter corresponds to $\phi_s^{eff} = 0.365$ which is less than $\phi_s = 0.4$.
- This indicates enhanced aggregation in active particles due to passive particles.

Cluster Size Distributions (CSD)

- For small ϕ_s , $p_s(n)$ has an exponential decay for large n .
- for large ϕ_s, it exhibits power law behaviour for all n .

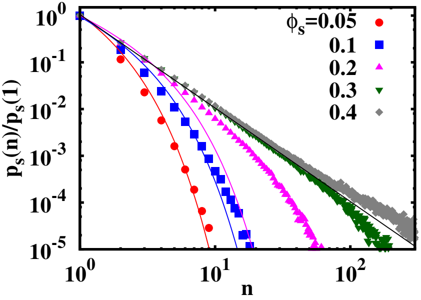

Figure: CSD of active particles for different ϕ_s at fixed $\phi_b = 0.076$ and $s = 5$.

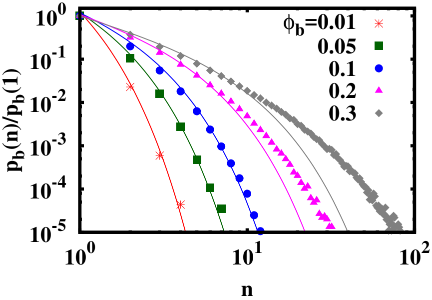

Figure: CSD of passive particles for different ϕ_b at fixed $\phi_s = 0.5$ and $s = 1.4$.

- Passive particles show more clustering as ϕ_b increases.
- $p_b(n)/p_b(1)$ fits to $f(n) = exp(-n/n_0)/n$ for small ϕ_b and deviates considerably from it for large ϕ_b .

CSD for different size ratios

- Clustering of passive particles is more for smaller size ratios (adjacent CSDs are for $\phi_s = \phi_b = 0.3$).
- $p_b(n)/p_b(1)$ fits to $f(n)$ for large s and deviates from it for small s .

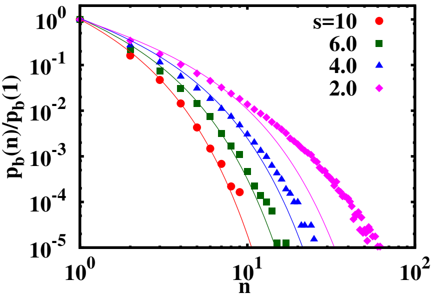

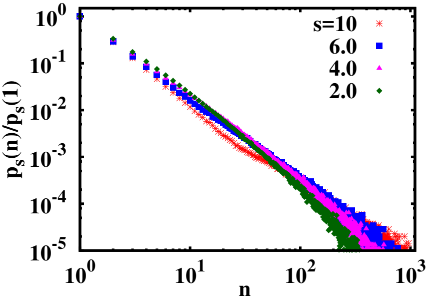

- Small clusters are more probable for small s .
- Large clusters are more probable for large s .
- Small passive particles hamper the formation of large clusters.
- Large passive particles enhance active particle clustering.

Summary

- There is an attraction between big passive particles, which is larger for large density and activity of active particles.
- In the dilute phase velocity distribution of passive particles scales with activity.
- Velocity distribution of active particles has a small hump indicating less mobile clusters.
- The diffusivity of passive particles increases almost linearly with size and activity and deviates from it for large size ratios.
- Passive particles exhibit giant number fluctuations when the volume fraction of active particles is sufficiently large.
- The CSD of active particles exhibit power law behaviour for large ϕ_s .
- Passive particles act as nucleation sites and enhance the clustering of active particles.

THANK YOU

List of publications

- Large deviation statistics of non-equilibrium fluctuations in a sheared model-fluid,
  Pritha Dolai and Aditi Simha,
  J. Stat. Mech. 083203 (2016).

- Universal spatio-temporal scaling of distortions in a drifting lattice,
  Pritha Dolai, Abhik Basu and Aditi Simha,
  Phys. Rev. E **95**, 052115 (2017).

- Dynamics of passive particles in active medium,
  Pritha Dolai, Aditi Simha and Shradha Mishra,
  arXiv:1706:02968 (Under review).

Distortions of a drifting lattice in a dissipative medium

Introduction: Crowley instability

- Drag force experienced by a single sphere is $F_D = 6\pi\eta a U$.
- In the presence of a second sphere the effective drag force is reduced by the interaction of their flow fields. $F_D = 6\pi\eta a U\{1 - \frac{3}{4}(a/d_1)\}$.
- Drag reduction is more for center particle and it falls faster.

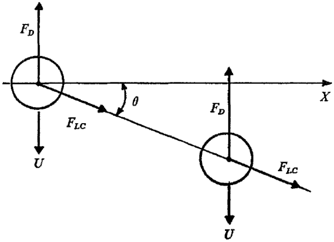

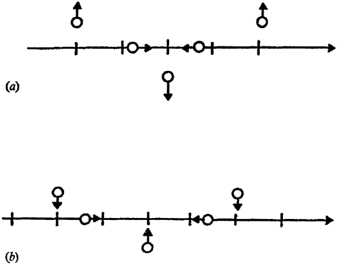

- Any small irregularity will be amplified by the viscous forces and the entire layer will break up into clumps of several particles.

Ref: J. M. Crowley, J. Fluid Mech.**45**, 151 (1971); Phys. Fluids **19**, 1296 (1976).

The equations of motion for displacement fields

- Ignoring inertia, the equations of motion for displacement fields $\mathbf{u}(\mathbf{r}, t)$ of a lattice drifting through a dissipative medium are of the form

$$\dot{\mathbf{u}} = \boldsymbol{\mu}.(\mathbf{F} + D\boldsymbol{\nabla}\boldsymbol{\nabla}\mathbf{u} + \mathbf{f})\,. \tag{4}$$

- The mobility tensor $\boldsymbol{\mu} = \boldsymbol{\mu_0} + A(\boldsymbol{\nabla} u) + O((\boldsymbol{\nabla} u)^2)\,.$

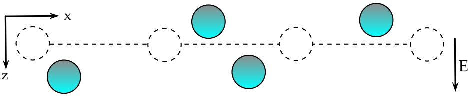

- The equation of motion retaining lowest order nonlinearities and gradients are

$$\dot{u}_x = \lambda_2 \partial_x u_z + \gamma_1 \partial_x u_x \partial_x u_z + D_1 \partial_x^2 u_x + f_x\,, \tag{5}$$

$$\dot{u}_z = \lambda_3 \partial_x u_x + \gamma_2 (\partial_x u_x)^2 + \gamma_3 (\partial_x u_z)^2 + D_2 \partial_x^2 u_z + f_z\,. \tag{6}$$

- Equations are invariant under $x \to -x$, $u_x \to -u_x$ but not under $u_z \to -u_z$.

Correlation functions

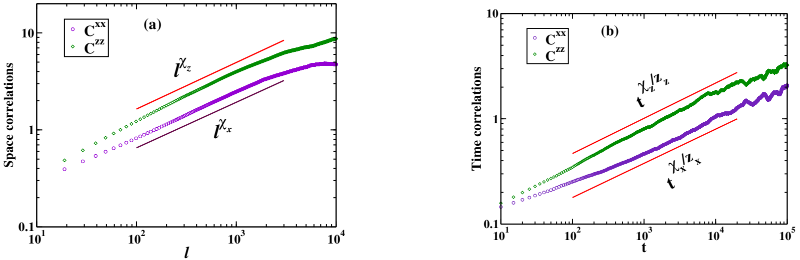

$$C^{xx}(x,t) = \langle u_x(x,t)u_x(0,0)\rangle = A_x|x|^{2\chi_x} f_x(t/x^{z_x})\,, \tag{7}$$

$$C^{zz}(x,t) = \langle u_z(x,t)u_z(0,0)\rangle = A_z|x|^{2\chi_z} f_z(t/x^{z_z})\,. \tag{8}$$

where χ_x , χ_z are roughness exponents and z_x , z_z are dynamic exponents.

Scaling exponents

- Dynamic RG calculations give $\chi_x = \chi_z = 0.5$ and $z_x = z_z = 1.5$ $[KPZ]$.
- Scaling exponents obtained from numerical simulations are
  $\chi_x = 0.47 \pm 0.06\,, \chi_z = 0.485 \pm 0.015\,.$
  $z_x = 1.45 \pm 0.05\,, z_z = 1.49 \pm 0.06\,.$
- Long-wavelength lattice distortions propagate as underdamped waves.
- In the drifting steady state, lattice distortions both transverse and longitudinal to the lattice, display strong dynamic scaling with dynamic exponent $3/2$.
- The system belongs to the KPZ (Kardar-Parisi-Zhang) universality class.
- The clumping instability seen in sedimentation does not exist in a colloidal crystal undergoing electrophoresis.

Pritha Dolai, Abhik Basu and Aditi Simha, *Phys. Rev. E.* **95**, 052115(2017).

Nonequilibrium fluctuations in a sheared model-fluid

1-D rotor model

- 1-D classical XY model with N rotors.

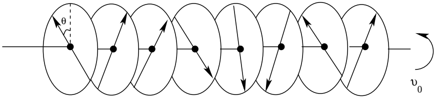

- Rotate in a plane perpendicular to the lattice but have no translational degrees of freedom.
- Driven away from equilibrium by forcing a constant relative velocity υ_0 between end two rotors.
- Thermostatted with a dissipative and random force (using Dissipative Particle Dynamics algorithm).
- The resulting steady state supports a velocity gradient in the system, closely mimicking a fluid under shear.
- Total force acting on the i-th rotor is given by

$$\mathbf{f}_i = \sum_{<ij>} \mathbf{F}_{ij}^C + \mathbf{F}_{ij}^D + \mathbf{F}_{ij}^R. \tag{9}$$

Model

- Forces act along $\hat{\theta}_{ij}$ where θ_{ij} is the relative angular separation between rotors i and j.

$$\mathbf{F}_{ij}^{C} = -\nabla U_{ij}\,,\ \mathbf{F}_{ij}^{D} = -\Gamma(\mathbf{v}_i - \mathbf{v}_j)\,,\ \mathbf{F}_{ij}^{R} = \sigma\zeta_{ij}\,. \tag{10}$$

- Γ is the friction co-efficient, σ is noise amplitude and ζ is a Gaussian random variable with unit variance.
- Strain rate $\dot{\gamma} = \upsilon_0/N$ and energy flux $\dot{W}(t) = f(t)\upsilon_0$.
- Average energy flux $\dot{W}_\tau = \frac{1}{\tau}\int_t^{t+\tau} \dot{W}(t')\,\mathrm{d}t' = f_\tau \upsilon_0$ and $P(\dot{W}_\tau/\upsilon_0) = P(f_\tau)$.
- Define a dimensionless quantity $\frac{f_\tau}{<f_\tau>} = \frac{W_\tau}{<W_\tau>} = X_\tau$.

Fluctuation Theorem (FT)

- FT provides a consistent thermodynamic description of small scale systems driven arbitrarily far from equilibrium.
- It gives an expression for the probability of entropy production in the direction opposite to that required by the second law of thermodynamics.
- The steady state Gallavotti-Cohen fluctuation theorem has the form

$$\lim_{\tau\to\infty} \frac{1}{\tau} \ln \frac{P(+W_\tau)}{P(-W_\tau)} = \beta W_\tau \tag{11}$$

  where $\beta = (k_B T_{eff})^{-1}$ defines an effective temperature.
- In terms of X_τ, fluctuation theorem for finite τ is

$$\ln(R) \equiv \ln \frac{P(+X_\tau)}{P(-X_\tau)} = \beta \langle W_\tau \rangle X_\tau \tau. \tag{12}$$

Results: Validate fluctuation theorem

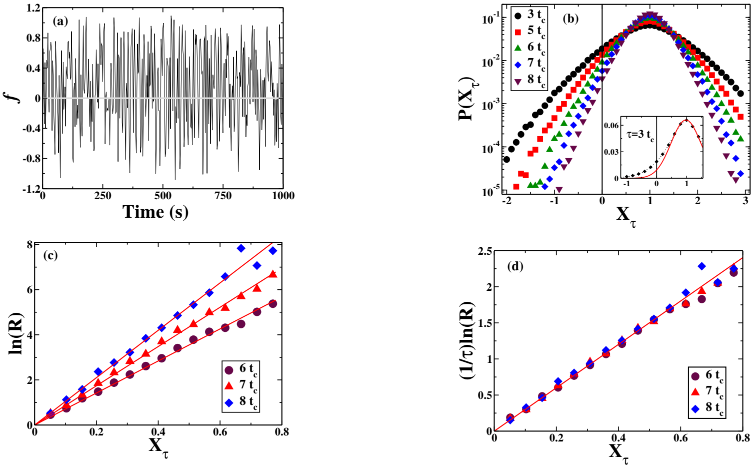

- Results with parameter values $\dot{\gamma}$=0.327 s^{-1}, $\sigma = 0.1$.

Phase Diagram

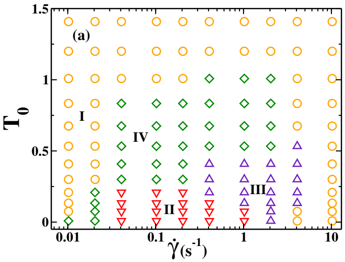

Figure: I - uniform shear flow,
II - slip plane phase,
III - solid-fluid coexistence phase,
IV - shear banding regime.

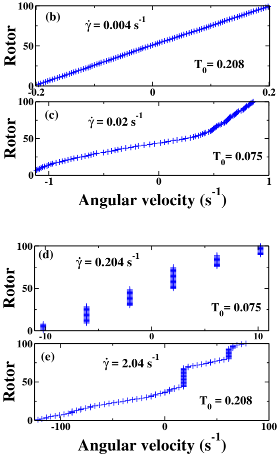

Figure: Velocity profiles in different phases

Pritha Dolai and Aditi Simha, *J. Stat. Mech*, 083203 (2016).

Variation of effective temperature

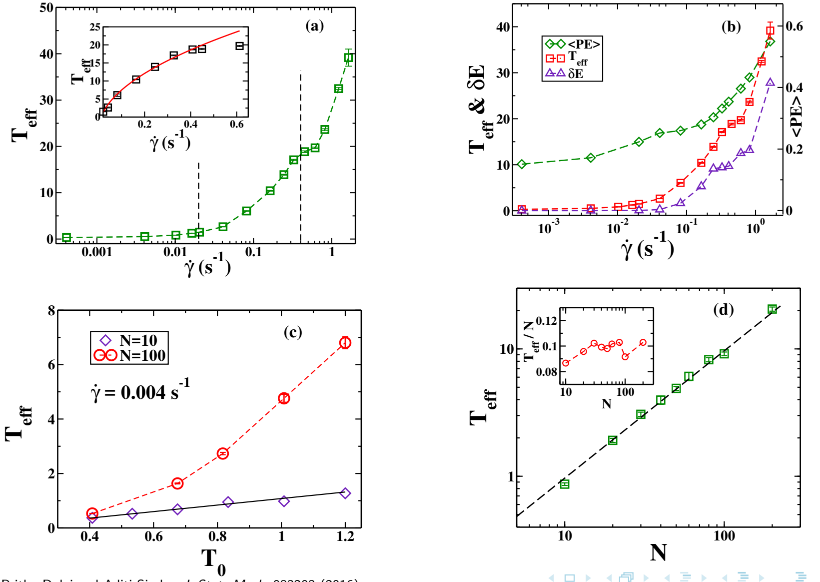

Pritha Dolai and Aditi Simha, *J. Stat. Mech*, 083203 (2016).

Statistics of local strain rate

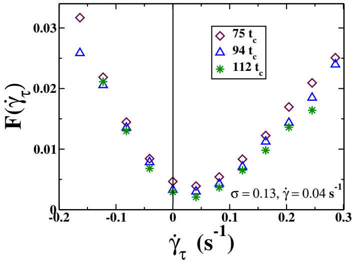

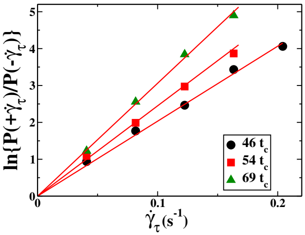

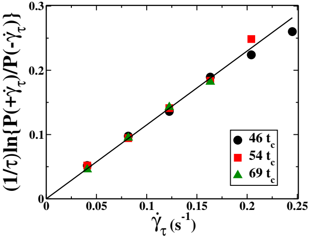

- The large deviation function (LDF) for the local strain rate is defined as $F(\dot\gamma_\tau) \equiv \lim_{\tau\to\infty} -(1/\tau)\ln P(\dot\gamma_\tau)$.
- The antisymmetric part of the LDF obeys a fluctuation relation.

LDFs for the local strain rate

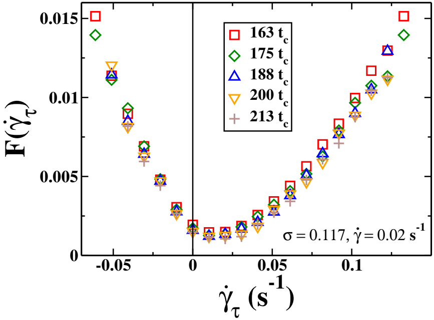

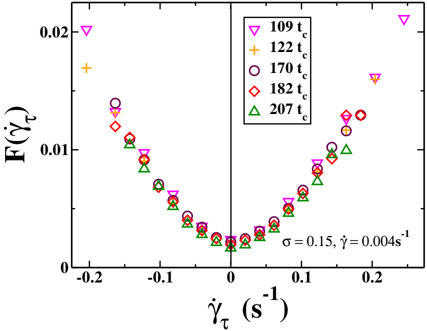

Summary

- Gallavotti-Cohen FT is satisfied across all phases of the sheared *model fluid*.
- In the linear response regime $T_{eff} \approx T_0$ for small system size and deviates considerably from T_0 for large σ and large system size.
- The dependence of T_{eff} on $\dot{\gamma}$ is phase-dependent.
- It doesn't change much at the phase boundaries.
- The local strain rate statistics obeys the large deviation principle and satisfies a fluctuation relation.
- It does not exhibit a distinct kink at zero strain rate, seen in other systems, because of the inertia of rotors in our system.